BEHAVIOR AND DESIGN OF HSC MEMBERS SUBJECTED TO AXIAL COMPRESSION AND FLEXURE

Halit Cenan Mertol, SungJoong Kim, Amir Mirmiran, Sami Rizkalla and Paul Zia

Synopsis: This paper identifies the fundamental design issues related to the behavior of high-strength concrete (HSC) members with compressive strengths up to 124 MPa (18 ksi) subjected to axial compression loads. The findings are based on critical assessment and synthesis of available data, the experiences of bridge owners, concrete fabricators, and current bridge design codes from North America, Europe, Australia, and Asia. The paper discusses the various factors believed to affect the design and behavior of HSC compression members, including the fundamental properties of concrete, member geometry, support conditions, main and lateral reinforcement, and type of construction. The significance of modeling of the stress-block, potential early spalling of concrete and reliability issues of HSC columns is also discussed. This paper represents the current efforts by the authors to recommend revisions to the AASHTO-LRFD Bridge Design Specifications, which currently limits the compressive strength of concrete to 69 MPa (10 ksi).

Keywords: column; combined compression and flexure; compression members; high-strength concrete; stress block parameters

Halit Cenan Mertol is a member of ACI. He obtained his BSCE (1999) and MSCE (2002) from Middle East Technical University in Turkey. He is currently a Ph. D. student in Civil, Construction and Environmental Engineering in North Carolina State University, Raleigh, North Carolina. His main interests are high-strength concrete and fiber reinforced polymer materials.

SungJoong Kim is a Ph. D. student in the Department of Civil, Construction and Environmental Engineering at North Carolina State University. He received his BS (1997) and MS (2000) degrees from the Dept. of Civil and Environmental Engineering of Chung-Ang University, Seoul, Korea. His main research interests include the structural use of high-strength concrete and design of high-strength concrete columns.

Amir Mirmiran is Professor and Chair of the Department of Civil and Environmental Engineering at the Florida State International University in Miami, FL. He has served on the faculty of the North Carolina State University, University of Cincinnati and the University of Central Florida. His research interests include high-performance concrete and composite materials.

Sami Rizkalla is a Distinguished Professor of Civil and Construction Engineering in the Department of Civil, Construction and Environmental Engineering, North Carolina State University. He is the Director of the Constructed Facilities Laboratory and NSF I/UCRC in Repair of Structures and Bridges at North Carolina State University. He is a fellow of ACI, ASCE, CSCE, EIC and IIFC.

ACI member **Paul Zia** is a Distinguished University Professor Emeritus at North Carolina State University. He served as ACI president in 1989, and is a member of the ACI Committee 363, High-Strength Concrete; Concrete Research Council; and Joint ACI-ASCE Committee 423, Prestressed Concrete; and ACI Committee 445, Shear and Torsion.

INTRODUCTION

Development of high-strength concrete (HSC) dates back to 1930's, but these early developments were economically prohibitive for practical applications. In the 1960’s, superplasticizers were developed in Japan and Germany and made it possible to decrease the water-to-cement ratio of concrete while maintaining its workability. In the 1970’s, the combined use of super-plasticizers and ultra-fine materials such as silica fume, finely ground granulated blast furnace slag or anhydrous gypsum led to further improvement of concrete performance measures including its strength. Since the mid-1980’s, HSC has gained popularity in both precast and cast-in-place construction for either reinforced or prestressed members. In Japan, concrete strengths as high as 11.4 ksi (79 MPa) were used in the 1970’s for railway bridges (ACI 363R-92 1997).

In the early 1990's, the Federal Highway Administration (FHWA) began sponsoring the use of High Performance Concrete (HPC) in several demonstration projects. Since 1993, a number of HPC bridges have been constructed across the country. The FHWA compilation project (Russell et al. 2003) reports on 19 such bridges in 14 states. While the highest design concrete strength in these bridges was reported as 14 ksi (97 MPa) in Texas, the achieved strength at the design age reached as high as 15.9 ksi (110 MPa) in South Dakota.

The *AASHTO LRFD Bridge Design Specifications*, first published in 1994, includes an article (5.4.2.1) limiting its applicability to a maximum concrete strength of 10 ksi (69 MPa), unless physical tests are made to establish the relationship between concrete strength and its other properties. These limitations reflected the lack of research data at the time, rather than the inability of the material to perform its intended function. Many design provisions stipulated in the LRFD Specifications are still based on test results obtained from specimens with compressive strengths up to 6 ksi (41 MPa). Although such a strength limit is not explicitly imposed by other codes such as the ACI 318-02 (2002), except in the provisions for development length, their applicability to HSC is not fully addressed either.

The National Cooperative Highway Research Program has initiated four separate projects to expand the LRFD Specifications, allow broader use of HSC, and meet the needs of the bridge design community. The objective of NCHRP Project 12-64, which is the focus of this paper, is to recommend revisions to the LRFD Specifications to extend the applicability of its compressive and combined compressive and flexural design provisions for reinforced and prestressed concrete members to concrete strengths up to 18 ksi (124 MPa).

AFFECTING FACTORS FOR HIGH-STRENGTH CONCRETE

The factors that affect the compressive and combined compressive and flexural behavior of reinforced and prestressed high-strength concrete members were identified from the databank assembled by the authors.

Compressive Strength and Ultimate Strain of Concrete

The compressive strength of concrete directly affects the load carrying capacity of reinforced and prestressed concrete members subjected to compression and combined compression and flexure. However, there is not a common definition for HSC. The FHWA Compilation Report (Russell et al. 2003) suggests the following three grades: Grade 1 for 8 ksi (55 MPa) $\leq f'_c <$ 10 ksi (69 MPa), Grade 2 for 10 ksi (69 MPa) $\leq f'_c <$ 14 ksi (97 MPa) and Grade 3 for 14 ksi (97 MPa) $\leq f'_c$.

The stress-strain response of concrete, its compressive strength and its ultimate strain are functions of several parameters, including the mix proportions, type of cement and cementitious materials, type of admixtures, and type and grading of aggregates. Other factors that influence the compressive strength and ultimate strain of concrete include curing, specimen type and size, moisture content and end conditions of test specimens, specimen age at the time of testing, and rate of loading. Some parameters are known to affect certain properties of concrete more than others. For example, aggregate type has a profound effect on the elastic modulus of concrete.

Figure 1 shows typical axial stress-strain curves for a range of concrete compressive strengths up to nearly 16 ksi (110 MPa). As the concrete strength increases, the strain at the peak stress increases slightly, the shape of the ascending branch of the stress-strain curve becomes more linear and steeper, and the slope of the descending part also becomes steeper.

As seen in Figure 1 above, the effective (useable) ultimate strain of concrete decreases as the strength increases. All design codes in the U.S. suggest a conservative value of 0.003 for design, whereas some of the foreign codes (e.g., Belgium, Sweden, Germany, and Canada) use 0.0035. Codes in the U.K. use an ultimate strain of 0.0036 for a concrete compressive strength of 1.8 ksi (12 MPa), but gradually reduce it to 0.0028 for a concrete compressive strength of 7.3 ksi (50 MPa).

Modulus of Elasticity of Concrete

Modulus of elasticity of concrete affects the elastic deformation of reinforced and prestressed concrete members, lateral stiffness of columns, and the loss of prestress. The modulus increases with the strength, however, at a somewhat lower rate. The FHWA Compilation Report (Russell et al. 2003) suggests changing the limits of elastic modulus for different grades of concrete which are 5,000 ksi (34,475 MPa) $\leq E_c <$ 6,000 ksi (41,370 MPa) for Grade 1, 6,000 ksi (41,370 MPa) $\leq E_c <$ 7,000 ksi (48,265 MPa) for Grade 2 and 7,000 ksi (48,265 MPa) $\leq E_c$ for Grade 3.

Figure 2 shows over 300 available test results from the databank on the modulus of elasticity in comparison with the design expressions of the LRFD Specifications and ACI 363R-92 (1997), the latter of which follows the equation proposed by Carrasquillo et al. (1981).

Poisson's Ratio of Concrete

The Poisson's ratio affects lateral expansion of concrete, thereby influencing the effectiveness of the transverse reinforcement. The limited test data suggests a range of 0.20–0.28 for the Poisson's ratio of HSC between compressive strengths of 8 and 11.6 ksi

(55 and 80 MPa) (Perenchio and Khieger 1978). The predominant factor in this regard appears to be the water-to-cement ratio. The ACI 363R-92 (1997) recommends using the same Poisson's ratio for HSC as that of NSC in the elastic range.

Modulus of Rupture of Concrete

The modulus of rupture of concrete represents its flexural tensile strength. It affects cracking moment for concrete members, and therefore, influences the minimum flexural reinforcement that is required to prevent sudden failure of the beam under flexural loads. It also affects strain limits in prestressed concrete members.

The literature review suggests values for the modulus of rupture of HSC in the range of $0.24\sqrt{f'_c}$ to $0.38\sqrt{f'_c}$ ksi ($0.62\sqrt{f'_c}$ to $\sqrt{f'_c}$ MPa). Carrasquillo et al. (1981) suggested a higher value of $0.37\sqrt{f'_c}$ ($0.97\sqrt{f'_c}$ MPa) for concrete compressive strengths of up to 12 ksi (83 MPa). Figure 3 shows some of the experimental values of the modulus of rupture in comparison with different design codes and research publications.

Based primarily on a number of SHRP projects (Zia et al. 1993), Russell et al. (2003) has proposed a revision to the modulus of rupture equations in the LRFD Specifications to include an upper bound of $0.37\sqrt{f'_c}$ ksi ($0.97\sqrt{f'_c}$ MPa) and a lower bound of $0.24\sqrt{f'_c}$ ksi ($0.62\sqrt{f'_c}$ MPa) for concrete compressive strengths of up to 15 ksi (103 MPa).

Creep Properties of Concrete

Creep is the change in length of a concrete member under constant sustained axial load. Creep properties of concrete affect long-term deflections of concrete members. The amount and rate of creep depend on the mix proportions and the constituent materials of concrete, age and strength of concrete at the time of loading, length of time under load, size of the member, amount of non-prestressed reinforcement, and the ambient environment.

The FHWA compilation report (Russell et al. 2003) suggests the following three grades of concrete based on its specific creep (ultimate creep per unit stress), which are 0.52×10^3 /ksi (75 /MPa) $\geq C_c > 0.38 \times 10^3$ /ksi (55 /MPa) for Grade 1, 0.38×10^3 /ksi (55 /MPa) $\geq C_c > 0.21 \times 10^3$ /ksi (30 /MPa) for Grade 2 and 0.21×10^3 /ksi (30 /MPa) $\geq C_c$ for Grade 3.

Parrott (1969) reported that the total strain observed in a sealed HSC specimen under a sustained loading of 30% of its ultimate strength was the same as that of a sealed NSC specimen when expressed as a ratio of the short-term strain. On the other hand, recent research (Tadros et al. 2003) has indicated that HSC undergoes less ultimate creep than NSC, while its creep develops relatively more rapidly than in NSC.

Shrinkage Properties of Concrete

Drying shrinkage is a shortening that results from loss of moisture from the concrete. Shrinkage will affect the long-term deformation and cracking of concrete members.

According to ACI 363R-92 (1997), a relatively high initial rate of shrinkage has been reported for HSC, as compared to NSC. However, after drying for about 180 days, there is little difference between the shrinkage of HSC and NSC made with dolomite or limestone. The magnitude and rate of shrinkage depend on many factors including mix proportions and constituent materials of concrete, size of member, amount of nonprestressed reinforcement, curing procedure and duration, and the ambient environment.

DESIGN ISSUES FOR HIGH-STRENGTH CONCRETE

The design issues for high-strength in compression and combined compression and flexure of reinforced concrete members were identified from the databank assembled by the authors. Also, a detailed review of Section 5 of the LRFD Specifications and their historical development was performed to ensure a thorough understanding of the implications of using HSC in compression and combined compression and flexure.

Axial Resistance for Compression Members

This issue is primarily related to Article 5.7.2.1 which limits the maximum strain at the extreme concrete compression fiber to 0.003, Articles 5.7.4.4 and 5.7.4.5 of the LRFD Specifications which use 0.85 for the reduction factor for axial compression.

In order to evaluate the above equations in the LRFD Specifications, it is necessary to review their basis and historical development. It is generally understood that the strength of concrete in a member is different from that in a concrete cylinder. Therefore, the strength obtained from testing a concrete cylinder is often multiplied by a factor to account for this difference. This factor originated from the column tests of Richart et al. in the early 1930's, as

$$P_o = k_3 f'_c \left(A_g - A_{st}\right) + f_y A_{st} \qquad (1)$$

The k_3 parameter in the above equation can be obtained either from concentrically loaded column tests or from combined compressive and flexural tests. In this equation, it is assumed that longitudinal steel bars in the column (if any) yield when concrete reaches its peak stress of f'_c. This assumption is generally justified, as the strain ε_{co} corresponding to the peak stress is usually about 0.002.

For concentrically loaded columns with lateral steel reinforcement, P_o is taken as the first peak load that corresponds to the spalling of cover concrete. Figure 4 shows the experimental values of k_3 from all available tests of concentrically loaded columns in the databank as a function of the concrete compressive strength. There is clearly significant scatter in the test results. Moreover, a scarcity of test data for concrete strengths above 14 ksi (97 MPa) is apparent. Some of the scatter may be explained by the fact that different investigators have used different size cylinders in determining the concrete compressive strength f'_c. It is generally accepted that compressive strength of concrete measured on 4 x 8 in (102 x 203 mm) cylinders is about 1% to 5% higher than the strength measured from the 6 x 12 in (152 x 305 mm) cylinders (Carino 1994).

The k_3 parameter may also be determined from combined compressive and flexural tests in comparison with compression tests, i.e., cylinder tests, as below:

$$k_3 = \frac{\text{Maximum Concrete Stress in Combined Compressive and Flexural Tests}}{\text{Maximum Concrete Stress in Compression Cylinder Tests}} \qquad (2)$$

In these combined compressive and flexural tests, a C-shaped specimen is loaded with two axial compression loads at two different eccentricities to create a compression only cross section (Figure 5). While loading the bracket to failure, the neutral axis is maintained at the outside face of the specimen throughout the test. The maximum stress in the above equation is obtained from closely spaced, consecutive readings of strain data in these eccentric bracket tests. Subsequently, an approximate stress can be calculated for concrete at every strain level. The maximum value of the stress obtained in this step is then used in the k_3 calculations. Figure 6 shows the experimental values of k_3 that were obtained from the available combined compression and flexural tests in the databank.

A cursory comparison of Figures 4 and 6 shows that the values of k_3 obtained from concentrically loaded columns are generally lower than those from combined compression and flexural tests. This difference may be explained as follows:

- The cover concrete in columns fails due to instability long before crushing of core concrete. The connection plane between the core concrete and the cover concrete is especially weak when large amounts of longitudinal and transverse steel reinforcement are provided. Therefore, separation of the cover concrete at this plane from the core concrete may be triggered very easily before crushing of core concrete.

- In combined compression and flexural tests, deflection of the member is such that the compression side is always on the concave side of the column, which is the side that is susceptible to cover buckling and instability. The cover concrete on this side has a tendency to buckle towards the core concrete, and therefore, is constrained against such instability. As a result, cover buckling is not an issue in members under bending.

- The quality of cover concrete is generally lower than the core concrete, simply because of inadequate compaction of the cover concrete especially for HSC mixes with low workability. Moreover, there is a difference between the drying shrinkage of the core concrete and that of the cover concrete.

- Low permeability of HSC leads to drying shrinkage strain in the cover concrete, while the core remains relatively moist. As a result, tensile stresses are developed in the cover concrete of HSC columns more rapidly than those in NSC columns.

In summary, the design issue of factored axial resistance is of great significance and of high priority. There is adequate test data to establish the necessary parameters described above. However, due to large scatter of the available test data and the scarcity of data for concrete compressive strengths above 14 ksi (97 MPa), validation tests are needed.

Behavior of Concrete in Compression Zones using Rectangular Stress Distribution

This issue is primarily related to Article 5.7.2.1 which limits the maximum strain at the extreme concrete compression fiber to 0.003 and Article 5.7.2.2 which defines the stress block parameters, while it also affects the flexural resistance in Article 5.7.3 of the LRFD Specifications.

As discussed earlier, the axial stress-strain relationship of concrete varies with its strength. The ascending and descending portions of the curve become steeper with increasing strength. The curves tend to become more linear for higher strength concretes. As a result, the equivalent stress block for high-strength concrete is expected to be different from that of normal-strength concrete.

A generalized stress block is defined by three parameters, k_1, k_2 and k_3. The design values of the stress block parameters are determined at the ultimate strain ε_{cu}, which corresponds to the maximum moment of the section. These parameters are depicted in Figure 7. They originated from the eccentric bracket tests performed by Hognestad et al. in the 1950's. The k_1k_3 value and the k_2 value can be obtained from the equilibrium of the external and internal forces as follows:

$$\begin{aligned} P_n &= k_1 k_3 f'_c bc + A_s' f_{su} + A_s f_{su} \\ M_n &= k_1 k_3 f'_c bc(d - k_2 c) + A_s' f_{su}(d - d') \end{aligned} \tag{3}$$

The three-parameter generalized stress block can be reduced to a two-parameter equivalent rectangular stress block, by keeping the resultant of the compression force at the mid-depth of the assumed rectangular stress block. The two parameters of α_1 and β_1 can be defined as

$$\alpha_1 = \frac{k_1 k_3}{2k_2} \qquad (4)$$
$$\beta_1 = 2k_2$$

The nominal axial and flexural resistance of the section can then be shown as:

$$P_n = \alpha_1 \beta_1 f'_c bc + A_s' f_{su} + A_s f_{su} \qquad (5)$$
$$M_n = \alpha_1 \beta_1 f'_c bc\left(d - \frac{\beta_1 c}{2}\right) + A_s' f_{su}(d - d')$$

Table 1 shows how the stress block parameters are treated in a number of different design codes. Table 2 shows the proposed equations in different reports and research publications. The ultimate compressive strain of concrete is also shown in these tables, as it affects the stress block parameters and the flexural resistance of the section.

Figures 8 through 10 show graphs of the experimental values of α_1 and β_1 obtained from eccentric bracket tests performed by Hognestad (1955), Nedderman (1973), Kaar (1976), Swartz (1985), Schade (1992) and Ibrahim and MacGregor (1996) and the product $\alpha_1\beta_1$ as a function of concrete compressive strength f'_c in comparison with different design codes. These results indicate that as the strength of concrete increases, $\alpha_1\beta_1$ decreases. These figures confirm earlier findings of the ACI 441R-96 (1996) that there are conflicting test results over the applicability of the current rectangular stress block approach to the columns made of HSC. While some studies have found the current approach for NSC columns to underestimate the flexural resistance of HSC columns at a given axial load, there are others who have found the approach to be quite un-conservative.

Reinforcement and Strain Limits for Compression Members

This issue is primarily related to Article 5.7.4 of the LRFD Specifications which limits the maximum and minimum reinforcement.

The equations in the LRFD Specifications are extrapolated for a range of concrete compressive strengths between 5 and 20 ksi (34 and 138 MPa), in the absence of any prestressing steel in the section. It was observed that the allowable longitudinal non-prestressing steel ratio ρ_l in a column to be between 4% to 8% for an 18 ksi (124 MPa) concrete and a Grade 60 ksi (414 MPa) steel. The upper bound is limited to 6% in seismic applications. Such high levels of minimum reinforcement would be quite unusual and need to be verified.

In order to evaluate these reinforcement limits, it is necessary to review their basis and historical development. Limits for longitudinal reinforcement in compression members originated from the early column tests by Richart et al. at the University of Illinois in 1930's. When a column is subjected to sustained service loads, the stress distribution between steel and concrete changes over time due to creep and shrinkage of concrete. With its creep and shrinkage progressing, concrete relieves itself from its initial share of the axial load. As a result, longitudinal steel reinforcement carries a larger portion of the sustained load over time. Therefore, it is theoretically possible that in columns with small amounts of longitudinal reinforcement, the steel could yield, resulting in creep rupture of the column. Tests by Richart et al. (1931-1933) showed the increase of stress in steel reinforcement to be inversely proportional to the percentage of the longitudinal steel. Results from these tests that were carried out on a range of concrete strengths between 2 and 8 ksi (14 and 55 MPa), indicated that a minimum reinforcement ratio of 1% was appropriate. The upper limit was initially established based on practical considerations of concrete placement, and has since been maintained for all ranges of concrete strengths.

The same rational procedure of Richart et al. (1931-1933) can be followed to establish the minimum reinforcement limits for HSC columns. Since creep properties of HSC are expected to be different from the NSC, the reinforcement limits are also expected to be changed. Using the same safety factors and the same duration of sustained loads as those in the early study of Richart et al. (1931-1933), the lower reinforcement limits can be rationally established for HSC with any combination of mild and prestressing steel.

The two strain limits of concern in compression members are the ultimate strain ε_{cu} of concrete at the ultimate limit state, and the strain ε_{co} of concrete corresponding to its peak stress f'_c. Figure 11 shows the variation of ε_{cu} as a function of f'_c. These results are obtained from tests on columns, beams, and cylinders. A review of the literature indicates that as the strength of concrete increases, ε_{cu} decreases. However, the figure shows that the current value of 0.003 for ε_{cu} in the LRFD Specifications remains valid for HSC.

Figure 12 shows the variation of ε_{co} as a function of f'_c, using all available results in the databank from tests on columns, beams, and cylinders. The figure clearly shows that as the strength of concrete increases, the strain at peak stress also increases. This has a profound effect on determining the axial resistance of compression members, since with higher ε_{co} the assumption of yielding of longitudinal steel reinforcement is well justified. It is not expected that the above strain limits for HSC compression members will change.

Confinement and Lateral Reinforcement

This issue is primarily related to Articles 5.7.4.6 and 5.10.11.4.1d of the LRFD Specifications which limits the volume ratio of the spiral reinforcement and the total gross sectional area of rectangular hoop reinforcement.

Transverse reinforcement in columns provides a passive form of confinement for concrete, as the lateral steel reacts to the expansion of concrete. Since HSC is expected to undergo less internal micro-cracking, its lateral strains are less than those seen in NSC columns. For that reason, a number of research experiments have shown the confinement reinforcement to be less effective in HSC columns, as compared to NSC columns. Therefore, lateral confinement pressure required for HSC columns may be significantly higher than that for NSC columns. The higher level of confinement pressure may be achieved using higher grades of lateral steel to avoid congestion of the reinforcement cage. On the other hand, HSC has been slow to gain acceptance in seismic regions due to its more brittle behavior in compression than the NSC.

The parameters that affect the confinement of concrete include yield strength, spacing, size, distribution, shape, and effectiveness of the confinement reinforcement, as well as distribution and yield strength of the longitudinal reinforcement, spalling of cover concrete, and level of axial load on the section.

The strength of confined concrete f_{cc} can be written as

$$f_{cc} = f'_c + C\sigma_2 \qquad (6)$$

Subsequently, the minimum volumetric ratio of spiral reinforcement can be found as

$$\rho_{s\min} = \frac{2}{C}\left[\frac{f'_c\,(A_g - A_{st} - A_c)}{f_{yw}A_c}\right] \qquad (7)$$

Equation (7) leads to Equation (5.7.4.6-1) in the LRFD Specifications using a value of 4.44 for the *C* parameter. It should be noted that the tests by Richart et al. (1928) identified the *C* parameter as 4.1 for NSC columns. Table 3 provides a summary of the confinement equations proposed in different research publications. Table 4 summarizes the minimum confinement reinforcement ratios specified in design codes or proposed in various research publications.

CONCLUSIONS

The design issues for normal-strength concrete must be verified and extended for high-strength concrete. There is available test data to establish the necessary parameters described above. However, because of the large scatter of the available test data and the scarcity of data for concrete compressive strengths above 14 ksi (97 MPa), validation tests are needed. After these validation tests, the revisions to the LRFD Specifications to extend the applicability of its flexural and compression design provisions for reinforced and prestressed concrete members to concrete strengths up to 18 ksi (124 MPa) will be recommended. The recommended provisions should be seamless and unified over the full range of concrete strengths.

ACKNOWLEDGEMENTS

The authors would like to acknowledge the support of the NCHRP through the project 12-64 and the Senior Program Officer, David Beal. The authors also thank the contributions of Dr. Henry Russell of Henry Russell, Inc. and Robert Mast of Berger/ABAM Engineers, Inc. who also serve as consultants on the project. The findings and the conclusion reported here are however of a preliminary nature and are those of the authors alone, and not necessarily those of the supporting agency.

REFERENCES

AASHTO LRFD Bridge Design Specifications, Second Edition, American Association of State Highway and Transportation Officials, Washington DC, 1998.

ACI Committee 318, "Building Code Requirements for Structural Concrete (ACI 318-02) and Commentary (318R-02)," American Concrete Institute, Farmington Hills, MI, 2002, 443 pp.

ACI Committee 363, "State-of-the-Art Report on High-Strength Concrete (ACI 363R-92)," American Concrete Institute, Detroit, MI, 1992 (Revised 1997), 55 pp.

ACI Committee 363, "Guide to Quality Control and Testing of High-Strength Concrete (ACI 363.2R-98)," American Concrete Institute, Detroit, MI, 1998, 18 pp.

Ansari, F. and Li, Q., "High Strength Concrete Subjected to Triaxial Compression," *ACI Materials Journal*, Vol. 95, No. 6, 1998, pp. 747-755.

Attard, M. M. and Setunge, S., "Stress-Strain Relationship of Confined and Unconfined Concrete," *ACI Structural Journal*, Vol. 93, No. 5, 1996, pp. 432-442.

Attard, M. M. and Stewart, M. G., "A Two Parameter Stress Block for High Strength Concrete," *ACI Structural Journal*, Vol. 95, No. 3, 1998, pp. 305-317.

Azizinamini, A., Kuska, S. S. B., Brungardt, P. and Hatfield, E., "Seismic Behavior of Square High-Strength Concrete Columns," *ACI Structural Journal*, Vol. 91, No. 3, 1994, pp. 336-345.

Bae, S. and Bayrak, O., "Stress Block Parameters for High-Strength Concrete Members," *ACI Structural Journal*, Vol. 100, No. 5, 2003, pp. 626-636.

Bayrak, O. and Sheikh, S. A., "Confinement Reinforcement Design Considerations for Ductile HSC Columns," *Journal of Structural Engineering*, Vol. 124, No. 9, 1998, pp. 999-1010.

Bing, L., Park, R. and Tanaka, H., "Stress Strain Behavior of High Strength Concrete Confined by Ultra-High- and Normal-Strength Transverse Reinforcement," *ACI Structural Journal*, Vol. 98, No. 3, 2001, pp. 395-406.

Canadian Standards Association, "Design of Concrete Structures, CSA A23.3 1994," Rexdale, Ontario, 1994, 199 pp.

Carino, N. J., "Prediction of Potential Strength at Later Ages," *Concrete and Concrete-Making Materials*, 1994, 140 pp.

Carrasquillo, R. L., Nilson, A. H. and Slate, F., "Properties of High Strength Concrete Subject to Short- Term Loads," *ACI Structural Journal*, Vol. 78, No.3, 1981, pp. 171-178.

Carrasquillo, R. L., Slate, F. and Nilson, A. H., "Micro-Cracking and Behavior of High Strength Concrete Subject to Short- Term Loading," *ACI Structural Journal*, Vol. 78, No.3, 1981, pp. 179-186.

Comite European de Normalisation (CEN), "Eurocode 2 : Design of Concrete Structures, Part 1 – General Rules and Rules for Buildings," prEN 1992-1, 2002, 211 pp.

Cusson, D. and Paultre, P., "High-Strength Concrete Columns Confined by Rectangular Ties," *Journal of Structural Engineering*, Vol. 120, No. 3, 1994, pp. 783-804.

Dahl, K. K. B., "Uniaxial Stress-Strain Curves for Normal and High-Strength Concrete," *ABK Report No. R282*, Department of Structural Engineering, Technical University of Denmark, 1992.

Dong Z. and Keru, W., "Fracture Properties of High-Strength Concrete," *Journal of Materials in Civil Engineering*, Vol. 13, No. 1, 2001, pp. 86-88.

Ho, J. C. M. and Pam, H. J., "Inelastic Design of Low-Axially Loaded High Strength Concrete Reinforced Columns," *Engineering Structures*, Vol. 25, No. 8, 2003, pp.1083-1096.

Hognestad, E., Hanson, N. W. and McHenry, D., "Concrete Stress Distribution in Ultimate Strength Design," ACI Journal, Vol. 52, No. 4, 1955, pp. 455-479.

Ibrahim, H. H. H. and MacGregor, G., "Tests of Eccentrically Loaded High-Strength Concrete Columns," *ACI Structural Journal*, Vol. 93, No. 5, 1996, pp. 585-594.

Ibrahim, H. H. H. and MacGregor, G., "Modification of the ACI Rectangular Stress Block for High-Strength Concrete," *ACI Structural Journal*, Vol. 94, No. 1, 1997, pp. 40-48.

Iravani, S., "Mechanical Properties of High-Performance Concrete," *ACI Materials Journal*, Vol. 93, No. 5, 1996, pp. 416-426.

Issa, M. A. and Tobaa, H., "Strength and Ductility Enhancement in High-Strength Confined Concrete," *Magazine of Concrete Research*, Vol. 46, No. 168, 1994, pp. 177-189.

Kaar, P. H., Hanson, N. W. and Capell, H. T., "Stress-Strain Characteristics of High Strength Concrete," *ACI Special Publication-55*, Douglas McHenry International Symposium on Concrete and Concrete Structures, Michigan, MI, 1978, pp. 161-185.

Kahn, L. F. and Meyer, K. F., "Rectangular Stress Block for Non-rectangular Compression Zone," *ACI Structural Journal*, Vol. 92, No. 3, 1995, pp. 304-310.

Li, B., "Strength and Ductility of Reinforced Concrete Members and Frames Constructed Using High Strength Concrete," *Ph. D. Thesis in Civil Engineering*, University of Canterbury, Christchurch, New Zealand, 1993.

Legeron, F. and Paultre, P., "Prediction of Modulus of Rupture of Concrete," *ACI Materials Journal*, Vol. 97, No. 2, 2000, pp. 193-200.

Legeron, F. and Paultre, P., "Behavior of High-Strength Concrete Columns under Cyclic Flexure and Constant Axial Load," *ACI Structural Journal*, Vol. 97, No. 4, 2000, pp. 591-601.

Le Roy, R., "Instantaneous and Time Dependant Strains of High-Strength Concrete," Laboratoire Central des Ponts et Chaussees, Paris, France, 1996, 376 pp.

Liu, J., Foster, S. J. and Attard, M. M., "Strength of Tied High Strength Concrete Columns Loaded in Concentric Compression," *ACI Structural Journal*, Vol. 97, No. 1, 2000, pp. 149-156.

Nedderman, H., "Flexural Stress Distribution in Very-High Strength concrete," *M.Sc. Thesis*, University of Texas at Arlington, 1973, 182 pp.

Noguchi Laboratory Data, Department of Architecture, University of Tokyo, Japan, (http://bme.t.u-tokyo.ac.jp/index_e.html).

Ozbakkaloglu, T. and Saatcioglu, M., "Rectangular Stress Block for High-Strength Concrete," *ACI Structural Journal*, Vol. 101, No. 4, 2004, pp. 475-483.

Parrot, L. J., "The Properties of High-Strength Concrete," *Technical Report No. 42.417*, Cement and Concrete Association, Wexham Springs, 1969, 12 pp.

Paultre, P. and Mitchell, D., "Code Provisions for High-Strength Concrete - An International Perspective," *Concrete International*, 2003, pp. 76-90.

Razvi, S. R. and Saatcioglu, M., "Confinement Model for High Strength Concrete," *Journal of Structural Engineering*, Vol. 125, No. 3, 1999, pp. 281-289.

Pendyala, R. and Mendis, P. A., "A Rectangular Stress Block for High Strength Concrete," Structural Engineering Journal, Institution of Engineers, Australia, Vol. CE39, No. 4, 1998, pp.135-144.

Perenchio, W. F. and Khieger, P., "Some Physical Properties of High Strength Concrete," *Research and Development Bulletin No. RD056.01T*, Portland Cement Association, Skokie, IL, 1978, 7 pp.

Richart, F. E., Brandtzaeg, A. and Brown, R. L., "A Study of the Failure of Concrete under Combined Compressive Stresses," *Bulletin 185*, University of Illinois Engineering Experiment Station, Urbana, Illinois, 1928, 104 pp.

Richart, F. E. and Staehle, G. C., "Progress Report on Column Tests at the University of Illinois," *Journal of American Concrete Institute*, Vol. 27, 1931, pp. 731-760.

Richart, F. E. and Staehle, G. C., "Second Progress Report on Column Tests at the University of Illinois," *Journal of American Concrete Institute*, Vol. 27, 1931, pp. 761-790.

Richart, F. E. and Staehle, G. C., "Third Progress Report on Column Tests at the University of Illinois," *Journal of American Concrete Institute*, Vol. 28, 1931, pp. 167-175.

Richart, F. E. and Staehle, G. C., "Fourth Progress Report on Column Tests at the University of Illinois," *Journal of American Concrete Institute*, Vol. 28, 1932, pp. 279-315.

Richart, F. E., “Reinforced Concrete Column Investigation,” *Journal of American Concrete Institute*, Vol. 29, 1933, pp. 275-284.

Russell, H. G., Miller, R. A., Ozyildirim, H. C. and Tadros, M. K., “Compilation and Evaluation of Results from High Performance Concrete Bridge Projects, Volume 1,” *Federal Highway Administration*, 2003.

Russell, H. G., Miller, R. A., Ozyildirim, H. C. and Tadros, M. K., “Compilation and Evaluation of Results from High Performance Concrete Bridge Projects, Volume 2,” *Federal Highway Administration*, 2003.

Saatcioglu, M. and Baingo, D., “Circular High Strength Columns under Simulated Seismic Loading,” *Journal of Structural Engineering*, Vol. 125, No. 3, 1999, pp. 272-280.

Saatcioglu, M. and Razvi, S. R., “High Strength Concrete Columns with Square Sections under Concentric Compression,” *Journal of Structural Engineering*, Vol. 124, No. 12, 1998, pp. 1438-1447.

Schade, J. E., “Flexural Concrete Stress in High Strength Concrete Columns,” *M. S. Thesis in Civil Engineering*, the University of Calgary, Calgary, Alberta, Canada, 1992.

Swartz, S. E., Nikaeen, A., Narayan Babu, H. D., Periyakaruppan, N. and Refai, T. M. E., “Structural Bending Properties of Higher Strength Concrete,” *ACI Special Publication-87*, High-Strength Concrete, 1985, pp. 145-178.

Tadros, M., Al-Omaishi, N., Seguirant, J. S. and Galit, J. G., “Prestress Losses in Pretensioned High-Strength Concrete Bridge Girders,” *NCHRP Report 496,* Transportation Research Board*,* 2003.

Xie, J., Elwi, A. E. and MacGregor, J. G., “Mechanical Properties of Three High Strength Concretes Containing Silica Fume,” *ACI Structural Journal*, Vol. 92, No. 2, 1995, pp. 135-145.

Yong, Y. K., Nour, M. G. and Nawy, E. G., “Behavior of Laterally Confined High Strength Concrete under Axial Loads,” *Journal of Structural Engineering*, Vol. 114, No. 2, 1988, pp. 332-351.

Zia, P., Leming, M. L., Ahmad, S., Schemmel, J. J., Elliot, R. P. and Naaman, A. E., “Mechanical Behavior of High Performance Concrete, Vol. 1 – Vol. 5,” *SHRP Report C-361-365*, Strategic Highway Research Program, National Research Council, Washington, D. C., 1993.

LIST OF NOTATIONS

a: depth of equivalent rectangular stress block
A_1: area under bearing device,
A_c: area of core measured to the outside diameter of the spiral
A_g: gross cross-sectional area of member
A_{ps}: area of prestressing steel
A_s: area of tension reinforcement
A_{sh}: total cross-sectional area of tie reinforcement (including supplementary cross-ties)
A_{st}: total area of longitudinal steel
b: width of web, which is the same as the width of compression flange in rectangular sections
c: distance between the neutral axis and the extreme compression fiber
C: confinement effectiveness parameter.
C_c: specific creep
d: depth of tension steel from the extreme compression fiber
d': depth of compression steel from the extreme compression fiber
E_c: modulus of elasticity
e_x: eccentricity of the applied factored axial force in the X direction
e_y: eccentricity of the applied factored axial force in the Y direction
f'_c: specified compressive strength of concrete at 28 days, unless another age is specified
f'_{cc}: strength of confined concrete
f_{pe}: effective prestress after losses
f_{pu}: specified tensile strength of prestressing steel
f_{su}: ultimate strength of longitudinal steel
f_y: yield strength of longitudinal steel
f_{yh}: specified yield strength of spiral reinforcement,
h_c: core dimension
HSR: High-strength reinforcement
k_1: ratio of the average compressive stress to the maximum compressive stress
k_2: ratio of the depth of the resultant compressive force to the depth of neutral axis
k_3: ratio of the maximum compressive stress to the compressive strength of concrete cylinder f'_c.
m: modification factor.
M_n: nominal Flexural resistance of the section
NSR: normal-strength reinforcement
P_n: nominal axial resistance of the section
P_o: maximum load carried by an axially loaded member
P_{rx}: factored axial resistance determined on the basis that only eccentricity e_y is present
P_{ry}: factored axial resistance determined on the basis that only eccentricity e_x is present
P_{rxy}: factored axial resistance in biaxial flexure

s: vertical spacing of hoops (not exceeding 4 in)
α_1: reduction factor of concrete strength
β_1: stress block parameter
ε_{co}: strain of concrete corresponding to its peak stress f'_c.
ε_{cu}: strain of concrete at the ultimate limit state
ρ_l: allowable longitudinal non-prestressing steel ratio in a column
ρ_s: ratio of the volume of spiral reinforcement to the total volume of concrete core
ρ_{smin}: minimum volumetric ratio of spiral reinforcement
σ_2: equivalent lateral confining pressure for a spirally reinforced concrete column
φ: resistance factor for members in axial compression

Table 1 – Rectangular Stress Block Parameters in Different Design Codes

Reference	α_1	β_1	ε_{cu}
LRFD and ACI 318-02 (2002)	0.85	$0.85 \; for \; f'_c \leq 4\,ksi$ $0.85 - 0.05(f'_c - 4) \geq 0.65$ $for \; f'_c > 4\,ksi$	0.003
NZS 3101 (1995) (see Li, Park and Tanaka 1994)	$0.85 \; for \; f'_c \leq 8\,ksi$ $0.85 - 0.02758(f'_c - 8) \geq 0.75$ $for \; f'_c > 8\,ksi$	$0.85 \; for \; f'_c \leq 4.35\,ksi$ $0.85 - 0.05516(f'_c - 4.35) \geq 0.65$ $for \; f'_c > 4.35\,ksi$	0.003
CSA A23.3 (1994)	$0.85 - 0.01034 f'_c \geq 0.67$	$0.97 - 0.01724 f'_c \geq 0.67$	0.0035
EC2-02 (2002)	$\alpha_{cc} \; for \; f'_{ck} \leq 7.25\,ksi$ $\alpha_{cc}\left(1 - \frac{f'_{ck} - 7.25}{29}\right)$ $for \; 7.25\,ksi \leq f'_{ck} \leq 13.05\,ksi$	$0.80 \; for \; f'_{ck} \leq 7.25\,ksiI$ $0.80 - \frac{f'_{ck} - 7.25}{68}$ $for \; 7.25\,ksi \leq f'_{ck} \leq 13.05\,ksi$	$0.0035 \; for \; f'_{ck} \leq 7.25\,ksi$ $0.0026 + 0.035\left(\frac{13.05 - f'_{ck}}{14.5}\right)^4$ $for \; 7.25\,ksi \leq f'_{ck} \leq 13.05\,ksi$
NS 3473 (1995)			$0.0035 \; for \; f'_{ck} \leq 8\,ksi$
CEB-FIB (1990)	$0.85\left(1 - \frac{f'_c}{36.3}\right)$	1	$0.004 - 0.002\frac{f'_c}{14.5}$
AFREM (1995)	0.85	$1.0 - \left(\frac{0.7}{4.5 - 0.1724 f'_c}\right)$	0.003
ACI 441-R96 (1996)	$0.85 - 0.05033(f'_c - 10) \geq 0.60$ $for \; f'_c > 10\,ksi$	$0.67 \; for \; f'_c \geq 10\,ksi$	0.003

Table 2 – Proposed Rectangular Stress Block Parameters in Different Publications

Reference	α_1	β_1	ε_{cu}
Azizinamini et al. (1994)	$0.85\ for\ f'_c \le 10\,ksi$ $0.85 - 0.05(f'_c - 10) \ge 0.60$ $for\ f'_c > 10\,ksi$	$0.85\ for\ f'_c \le 4.35\,ksi$ $0.85 - 0.05516(f'_c - 4.35) \ge 0.65$ $for\ f'_c > 4.35\,ksi$	0.003
Ibrahim and MacGregor (1997)	$0.85 - \frac{f'_c}{116} \ge 0.725$	$0.95 - \frac{f'_c}{58} \ge 0.70$	0.003
Pendyala and Mendis (1998)	$0.85 - 0.01724(f'_c - 8.7)$ $for\ 8.7\,ksi \le f'_c \le 14.5\,ksi$	$0.65 - 0.00862(f'_c - 8.7)$ $for\ 8.7\,ksi \le f'_c \le 14.5\,ksi$	0.003
Attard and Stewart (1998)	$1.2932\left(\frac{f'_c}{0.145}\right)^{-0.0998} \ge 0.71\ for\ Dogbone\ Tests$ $0.6470\left(\frac{f'_c}{0.145}\right)^{0.0324} \ge 0.58\ for\ Sustain\ Load\ Tests$	$1.0948\left(\frac{f'_c}{0.145}\right)^{-0.091} \ge 0.67$	0.003
Bae and Bayrak (2003)	$0.85\ for\ f'_c \le 10.2\,ksi$ $0.85 - 0.02758(f'_c - 10.2) \ge 0.67$ $for\ f'_c > 10.2\,ksi$	$0.85\ for\ f'_c \le 4.35\,ksi$ $0.85 - 0.02758(f'_c - 4.35) \ge 0.67$ $for\ f'_c > 4.35\,ksi$	$0.003\ for\ f'_c \le 8\,ksi$ $0.0025\ for\ f'_c \ge 8\,ksi$
Ozbakkaloglu and Saatcioglu (2003)	$0.85\ for\ f'_c \le 4\,ksi$ $0.85 - 0.01(f'_c - 4) \ge 0.72$ $for\ f'_c > 4\,ksi$	$0.85\ for\ f'_c \le 4\,ksi$ $0.85 - 0.014(f'_c - 4) \ge 0.67$ $for\ f'_c > 4\,ksi$	0.003

Table 3 – Proposed Confinement Equations for NSC and HSC Columns

Reference	Proposed Equations
Richart (1928)	NSC: $f_{cc} = f'_c + 4.1\sigma_2$
Xie, Elwi and MacGregor (1995)	NSC and HSC: $\frac{f_{cc}}{f'_c} = \sqrt{1 + \left(21.2 - 0.05 f'_c\right)\left(\frac{\sigma_2}{f'_c}\right)}$
Attard and Setunge (1996)	NSC and HSC: $\frac{f_{cc}}{f'_c} = \left(\frac{\sigma_2}{f_t} + 1\right)^{1.25\left[1 + 0.062\frac{\sigma_2}{f'_c}\right](f'_c)^{-0.21}}$
Ansari and Li (1998)	NSC and HSC: $\frac{f_{cc}}{f'_c} = 1 + 2.45\left(\frac{\sigma_2}{f'_c}\right)^{0.703}$
Bing, Park and Tanaka (2001)	HSC, NSR, Rectilinear, Circular: $f_{cc} = f'_c + 4\sigma_2$ HSC, HSR, Circular: $f_{cc} = f'_c + 2.7\sigma_2$ HSC, HSR, Rectilinear: $f_{cc} = f'_c + 1.9\sigma_2$

Table 4 – Confinement Requirements in Different Design Codes and Publications

Reference	Requirement
LRFD Specifications and ACI 318-02 (2002)	$\rho_S \geq 0.45\left(\frac{A_g}{A_c} - 1\right)\left(\frac{f'_c}{f_y}\right)$ for spiral reinforcement $\rho_S \geq 0.12\frac{f'_c}{f_y}$ for spiral columns in seismic regions $A_{sh} \geq 0.30 s h_c\left(\frac{f'_c}{f_y}\right)\left[\frac{A_g}{A_c} - 1\right]$ for rectangular columns in seismic regions $A_{sh} \geq 0.12 s h_c\left(\frac{f'_c}{f_y}\right)$ for rect. col. in seismic regions for LRFD $A_{sh} \geq 0.09 s h_c\left(\frac{f'_c}{f_y}\right)$ for rect. col. in seismic regions for ACI 318-02
NZS 3101-95	$A_{sh} \geq \frac{\left(1.3 - \rho_g \frac{f_y}{0.85 f'_c}\right) s h''}{3.3}\left(\frac{A_g}{A_c}\right)\left(\frac{f'_c}{f_y}\right)\left(\frac{P}{\phi A_g f'_c}\right) - 0.006 s h''$
Ho and Pam (2003)	$\rho_S = \left(\frac{A_g}{A_c}\right)\left(0.2 - 0.2\frac{\rho_l f_y}{f_{cu}}\right)\left(\frac{P}{A_g f_{cu}}\right)^{0.9}\left(\frac{f_{cu}}{f_{yh}}\right) + 0.008$

Table 4 – Confinement Requirements in Different Design Codes and Publications (continued)

Saatcioglu and Baingo (1999)	$\rho_S \geq 0.17\frac{f'_c}{f_{yt}}$ for spiral, P = 0.43xP_0, $A_g/A_c - 1 = 0.23$ and 0.05 lateral drift
Razvi and Saatcioglu (1999)	$\rho_{S\min} \geq 0.09\frac{f'_c}{f_{yt}}$ for spiral, $A_g/A_c - 1 = 0.4$ $\rho_{Styp} \geq 0.14\frac{f'_c}{f_{yt}}$ for spiral, $A_g/A_c - 1 = 0.4$
Saatcioglu and Razvi (1998)	$\rho_{S\min} \geq 0.07\frac{f'_c}{f_{yt}}k_2$ for rectangular $\rho_{Styp} \geq 0.10\frac{f'_c}{f_{yt}}k_2$ for rectangular
Bayrak and Sheikh (1998)	$A_{sh} = \left[A_{sh(ACI)}\right]\alpha\left[1+13\cdot\left(\frac{P}{P_0}\right)^5\right]\left[\frac{(\mu_{\phi 80})^{0.82}}{8.12}\right]$

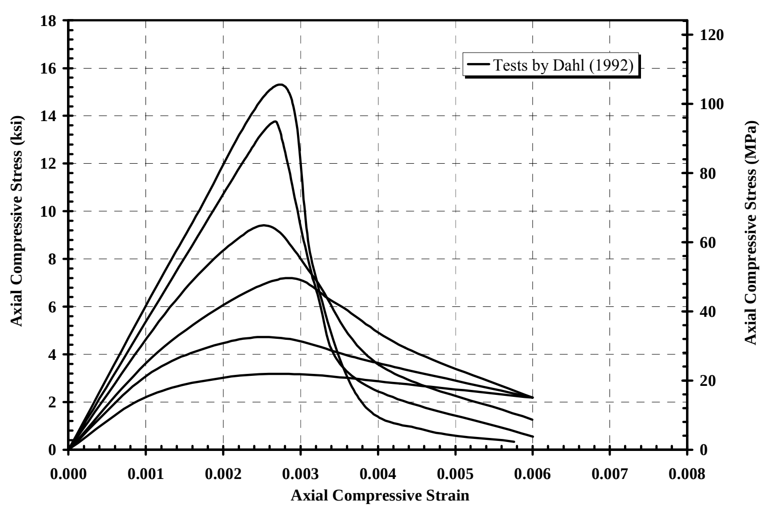

Figure 1 – Axial Compressive Stress-Strain Curves for Different Strengths of Concrete

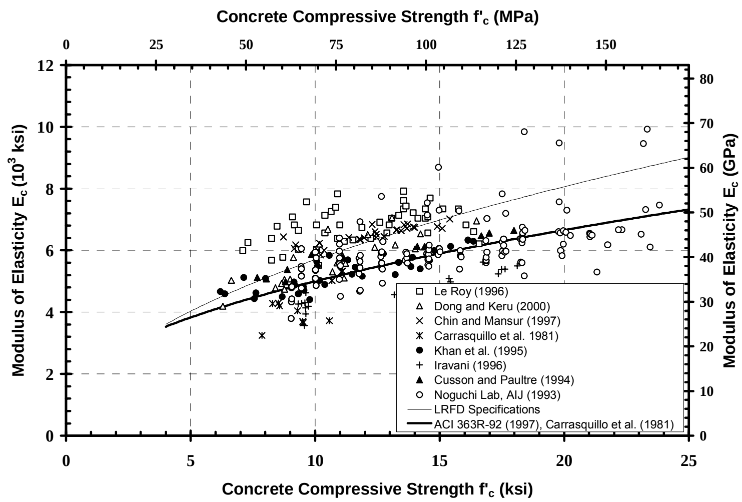

Figure 2 – Test Data and Design Expressions for Modulus of Elasticity of Concrete

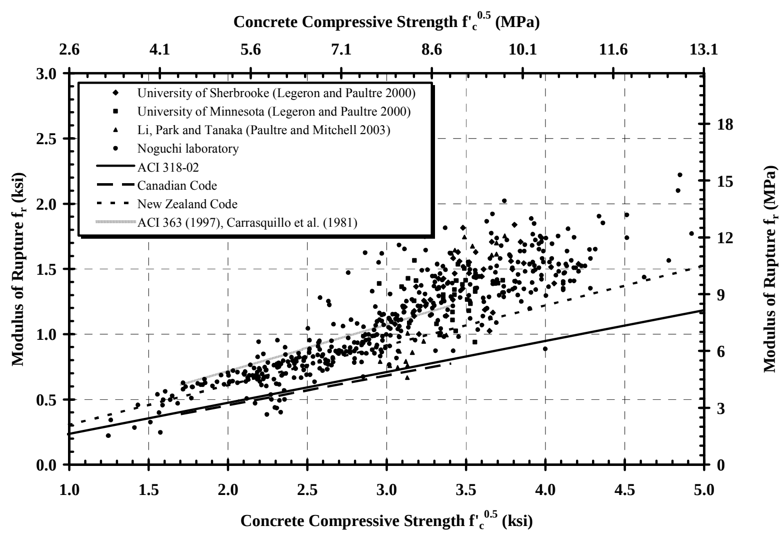

Figure 3 – Test Data and Design Expressions for Modulus of Rupture of Concrete

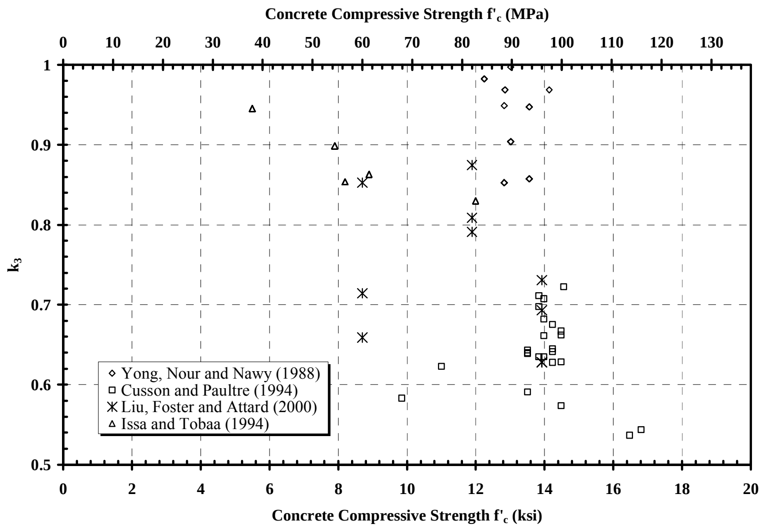

Figure 4 – k_3 Parameter from Concentrically Loaded Column Tests

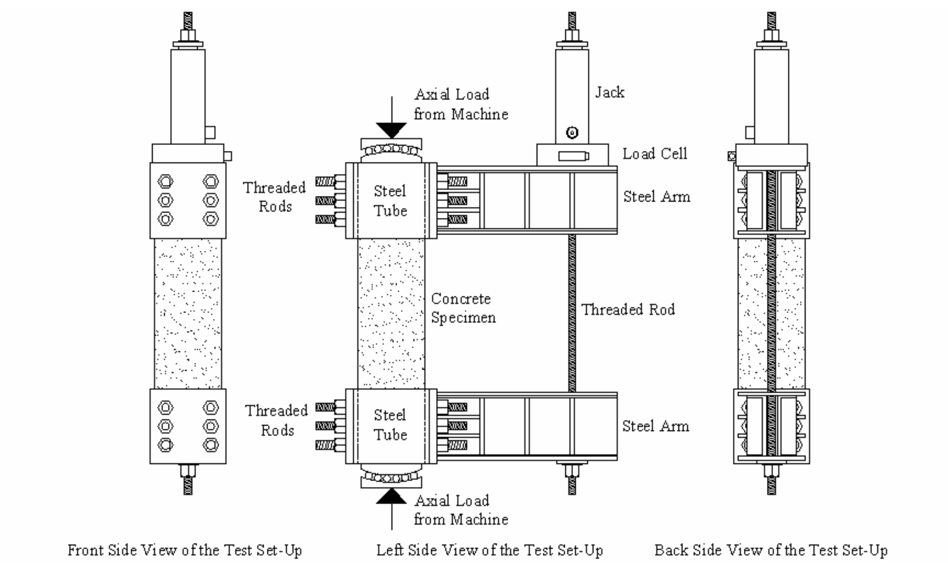

Figure 5 – C-Shaped Specimen

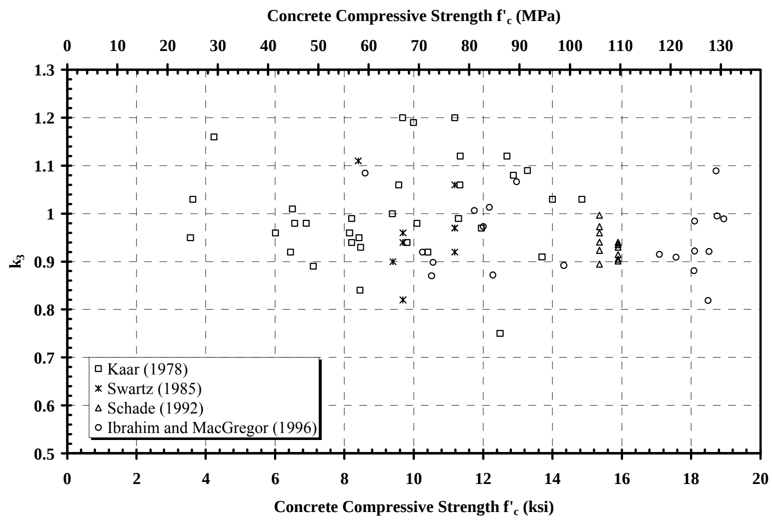

Figure 6 – k_3 Parameter from Combined Compressive and Flexural Tests

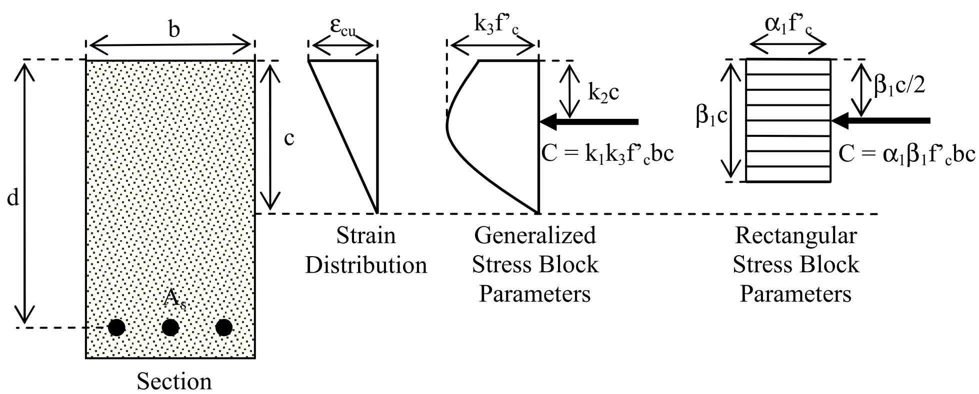

Figure 7 – Stress Block Parameters for Rectangular Sections

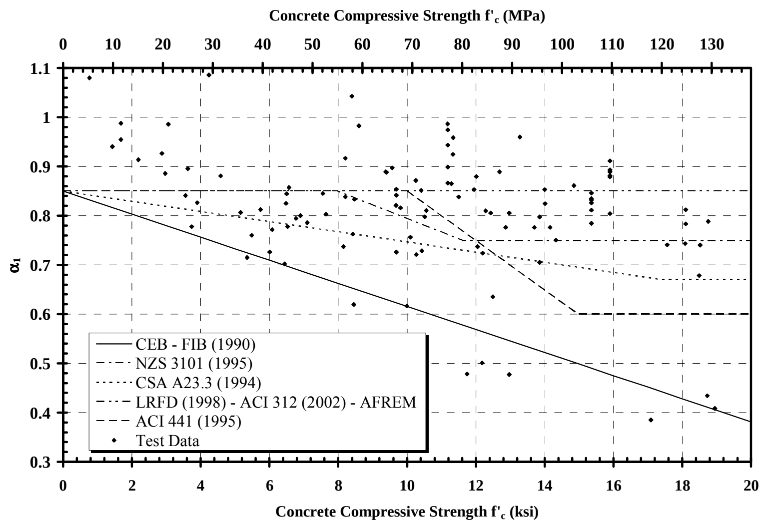

Figure 8 – Comparison of Experimental Values and Design Codes for α_1

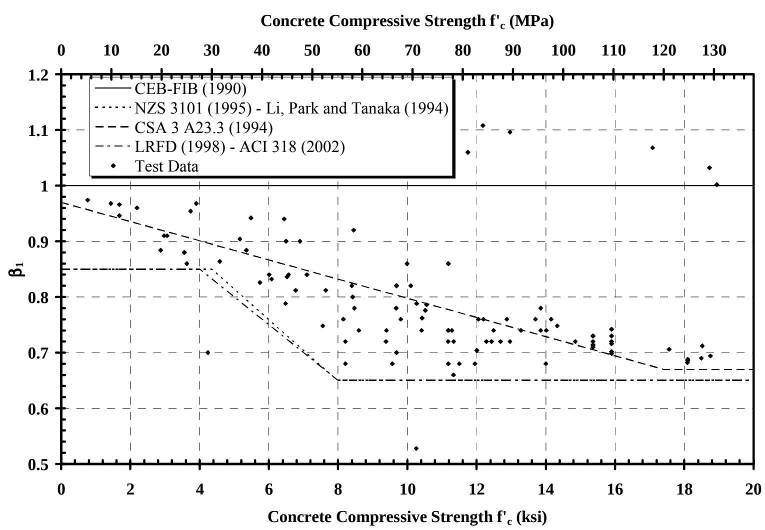

Figure 9 – Comparison of Experimental Values and Design Codes for β_1

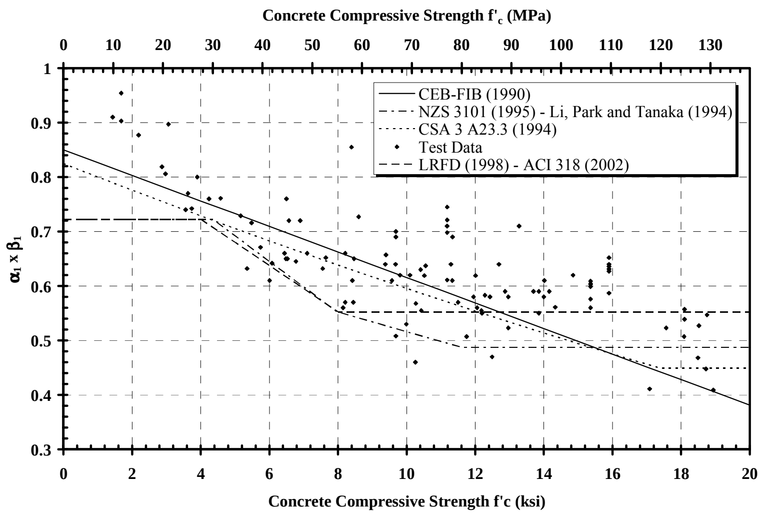

Figure 10 – Comparison of Experimental Values and Design Codes for $\alpha_1\beta_1$

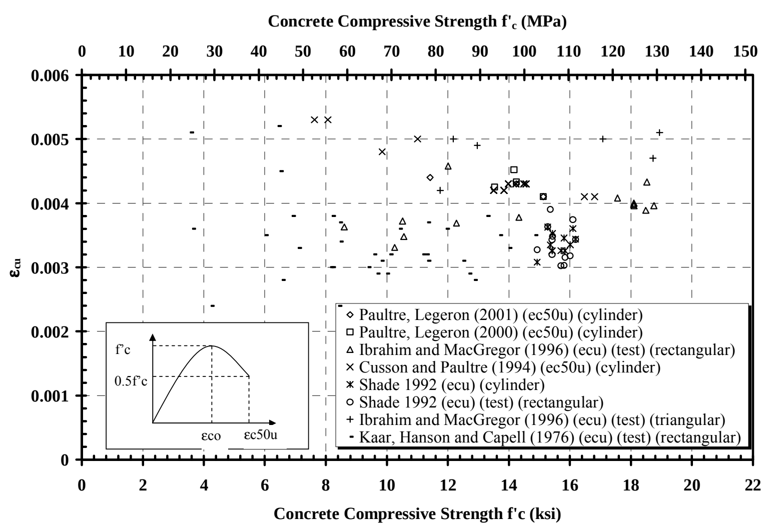

Figure 11 – Variation of ε_{cu} As a Function of f'_c

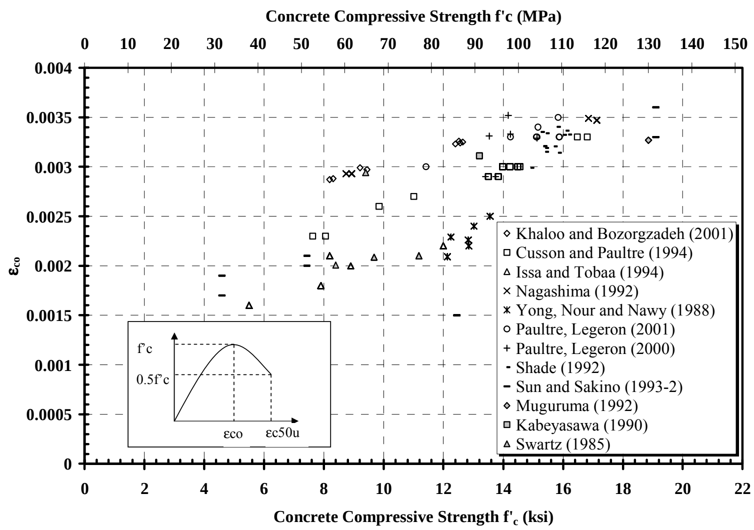

Figure 12 – Variation of ε_{co} As a Function of f'_c